

# Quantum-implementable selective reconstruction of high-resolution images

Mitja Peruš, Horst Bischof, H. John Caulfield, and Chu Kiong Loo

This paper, written for interdisciplinary audience, presents computational image reconstruction implementable by quantum optics. The input-triggered selection of a high-resolution image among many stored ones, and its reconstruction if the input is occluded or noisy, has been successfully simulated. The original algorithm, based on the Hopfield associative neural net, was transformed in order to enable its quantum-wave implementation based on holography. The main limitations of the classical Hopfield net are much reduced with the simulated new quantum-optical implementation. © 2004 Optical Society of America

OCIS codes: 090.0090, 100.3010, 200.4700, 200.4490, 270.0270.

## 1. Introduction

There is growing evidence that quantum-physical systems could be harnessed for information processing,<sup>1</sup> including image recognition,<sup>2</sup> in two ways: by Turing-machine-based quantum computing by use of quantum logic gates<sup>3–8</sup> and by quantum processing<sup>9</sup> similar to those in oscillatory associative neural nets<sup>10,11</sup> and holography.<sup>12</sup>

This interdisciplinary paper reports how it is possible, in principle, to implement successful image recognition, as verified by our simulations, in a quantum holographic process.<sup>13</sup> Since the natural fundamental quantum-wave dynamics is harnessed, it allows much easier and cheaper physical realization with much-bigger sizes and resolutions of images than the mainstream quantum-computing approaches.<sup>3–8</sup>

The main contribution of this paper is not to propose a generally better image-recognition method, but to present its potential alternative implementation into a quantum-wave medium (Section 2), and to demonstrate its plausibility by computational experiments (Section 3). Quantum-net's capacities of connectivity, parallelism, storage, associativity, speed, and miniaturization are enormous.

The Hopfield model with real-valued (thus not nec-

essarily binary) activities of units/neurons, having linear (not sigmoid or signum) activation function, can be transformed into a quantum-holographic procedure<sup>13,14</sup> where the Hebbian memory storage is replaced by multiple self-interferences of quantum plane waves. This translation<sup>15</sup> succeeded by the simplest variable exchange of the Hopfield's real-valued variables with the complex-valued variables changing as sinusoids (waves). Thereby, all input-to-output transformations are preserved. Thus quantum-wave image recognition functions equivalently to Hopfield's one; only the implementation is much miniaturized, enabling almost infinitely large associative memory.

Since the opposite translation, i.e., digitalization of holography, was done in the 1960s to get the first computational associative memories, one might wonder what is new in the present proposal. Additionally to the big experimental success of classical (optical, acoustic, microwave, x-ray, atom, and electron) holography,<sup>16</sup> the recent fast development of quantum optics<sup>17</sup> gave birth to quantum holography.<sup>13,14,18</sup> The latter might implement the well-known Hopfield model and its generalizations in a completely new framework in which the former obstacles (memory-capacity limitations, problems with nonorthogonality of small-size inputs producing cross talk) are very much reduced.

## 2. Hopfield Net and Quantum Holography

Using neuroquantum analogies<sup>19</sup> we transform the Hopfield-like associative neural net into quantum formalism:<sup>9,15</sup>

- Quantum wave-function  $\Psi$  acts as net's state vector  $\mathbf{q}$ .

M. Peruš ([perus@icg.tu-graz.ac.at](mailto:perus@icg.tu-graz.ac.at)) and H. Bischof are with the Institute for Computer Vision and Graphics, Graz University of Technology, Inffeldgasse 16 (2 O.G.), A-8010 Graz, Austria. H. John Caulfield is with Fisk University, 1800 17th Avenue North, Nashville, Tennessee 37208. C. K. Loo is with the Faculty of Engineering and Technology, Multimedia University–Melaka, MY-75450 Melaka, Malaysia.

Received 4 May 2004; revised manuscript received 13 August 2004; accepted 19 August 2004.

0003-6935/04/336134-05\$15.00/0

© 2004 Optical Society of America

- Quantum eigenwave functions  $\psi^k$  ( $k = 1, \dots, P$ ) act as Hopfield's pattern-bearing eigen-vectors (attractors)  $\mathbf{v}^k$ .

- The quantum Green-function propagator  $\mathbf{G}$  replaces the Hebb memory matrix  $\mathbf{J}$ .

- Thus sum of self-interferences  $\psi^k \otimes \psi^k$  of quantum waves  $\psi^k$  (the hologram  $\mathbf{G}$ ) implements the sum of autocorrelations of input-pattern configurations  $\mathbf{v}^k \otimes \mathbf{v}^k$  (the content-addressable associative memory  $\mathbf{J}$ ). ( $\otimes$  denotes tensor/outer product.)

The Hebb-equivalent expression for elements of  $\mathbf{G}$  (i.e.,  $\sum_k \psi^k \otimes \psi^k$ , which implements matrix  $\mathbf{J}$ ) is

$$G_{hj} = \sum_{k=1}^P \psi_h^k (\psi_j^k)^*, \quad (1)$$

where  $h$  and  $j$  denote the unit/pixel neuron at locations  $\mathbf{r}_1$  and  $\mathbf{r}_2$  at time  $t$  ( $h, j = 1, \dots, N$ ). The asterisk denotes a complex conjugation (optical analog, phase conjugation).

After we have succeeded in encoding images as eigenstates (attractors)  $\psi^k$  into the quantum system, preparing it using Eq. (1), we can reconstruct one image (e.g.,  $k_0^{\text{th}}$ ) by presenting a new input similar to the  $k_0^{\text{th}}$  stored one:

$$\begin{aligned} \Psi_h^{\text{output}} &= \sum_{j=1}^N G_{hj} \Psi_j^{\text{input}} \\ &= \sum_{j=1}^N \left[ \sum_{k=1}^P \psi_h^k (\psi_j^k)^* \right] \Psi_j^{\text{input}} \\ &= \sum_{k=1}^P \left[ \sum_{j=1}^N (\psi_j^k)^* \Psi_j^{\text{input}} \right] \psi_h^k \doteq \psi_h^{k_0} \end{aligned} \quad (2)$$

describes the resulting collapse-like selective retrieval (recognition) of image  $\mathbf{v}^{k_0}$  encoded in  $\psi^{k_0}$ .<sup>9,15</sup>

In the Dirac notation, Eq. (2) is, by use of  $(\mathbf{a} \otimes \mathbf{b})\mathbf{c} = \langle \mathbf{b}, \mathbf{c} \rangle \mathbf{a}$ :

$$\begin{aligned} |\Psi^{\text{output}}\rangle &= \mathbf{G} |\Psi^{\text{input}}\rangle \\ &= \left( \sum_k |\psi^k\rangle \langle \psi^k| \right) |\Psi^{\text{input}}\rangle \\ &= \sum_k \langle \psi^k | \Psi^{\text{input}} \rangle |\psi^k\rangle \doteq \psi^{k_0}. \end{aligned} \quad (3)$$

We assume that we can encode images  $\mathbf{v}^k$  into quantum plane waves:

$$\begin{aligned} \psi^k(\mathbf{r}, t) &= A^k(\mathbf{r}, t) \exp[i\varphi^k(\mathbf{r}, t)] \\ &= A^k \exp \left[ \frac{i}{\hbar} (\mathbf{p}^k \mathbf{r} - E^k t) \right]. \end{aligned} \quad (4)$$

For nonphysicists:  $\psi^k$  describes the sinusoidally changing probability distribution for measuring the  $k$ th mode of the photon with momentum  $\mathbf{p}^k$  and energy  $E^k$  at location  $\mathbf{r}$  at time  $t$  ( $\hbar$  is Planck's constant;  $i = \sqrt{-1}$ ).

We may choose the same constant amplitudes  $A$ , so that quantum phases (delays between wave peaks)  $\varphi$  encode the whole information. Let us

take  $A = 1$  (or  $A = 1/\sqrt{N}$  for convenient quantum normalization); therefore,  $A_j^k = 1$  for all  $k, j$ . The image-modulated laser beam is thus:  $\psi^k = [\exp(i\varphi_1^k), \exp(i\varphi_2^k), \dots, \exp(i\varphi_N^k)]$  where  $N$  is the number of wave-front peaks.

The neuro-quantum isomorphism<sup>15</sup> allows us to exchange variables,  $\mathbf{v}^k \leftrightarrow \exp(i\varphi^k)$  giving  $\psi_j^k = \exp(i\varphi_j^k)$  instead of Hopfield-like  $\psi_j^k = v_j^k$  (or  $\psi_j^k = A_j^k$ , respectively). With this exchange in Eqs. (1) and (2), all of the information-processing mathematics, verified by computer experiments in Section 3, remains valid for sinusoid-encoded images also. Namely, because Eq. (1) becomes

$$G_{hj} = \sum_{k=1}^P \exp(i\varphi_h^k) \exp(-i\varphi_j^k) = \sum_{k=1}^P \exp[i(\varphi_h^k - \varphi_j^k)]; \quad (5)$$

Eq. (2) becomes

$$\begin{aligned} &\exp(i\varphi_h^{\text{output}}) \\ &= \sum_{j=1}^N \left[ \sum_{k=1}^P \exp(i\varphi_h^k) \exp(-i\varphi_j^k) \right] \exp(i\varphi_j^{\text{input}}) \\ &= \sum_{k=1}^P \left[ \sum_{j=1}^N \exp(-i\varphi_j^k) \exp(i\varphi_j^{\text{input}}) \right] \exp(i\varphi_h^k) \\ &\doteq \exp(i\varphi_h^{k_0}). \end{aligned} \quad (6)$$

If the images are almost orthogonal, a wave carrying an image (those among many stored ones that is the most similar to the newly input one) is selectively reconstructed.

There is a nonlocal information exchange involved in this holographic process, which in our quantum case exploits the quantum interference array ( $\mathbf{G}$ ) itself, not its static imprint onto a crystal plate as in classical holography.

Our information-processing result could be extracted from  $\psi^{k_0}$  by use of new quantum-optical techniques such as

- wave packet reconstruction, sculpting, or engineering<sup>13,14</sup>
- quantum tomography<sup>20,21</sup>
- (coherent) quantum control and manipulation<sup>22</sup>
- quantum-phase estimation and engineering<sup>23</sup>

They are interrelated and often computer-aided.

$\Psi^{k_0}$  can be determined from a series of measurements on an ensemble of identically prepared systems (e.g., individual photons). Real-valued results from the measured observables are sufficient for (e.g., quantum-holographic<sup>13,14</sup>) reconstruction of the complex-valued wave function or density matrix. Phase-sensitive measurements, needed for that, have been experimentally realized on some systems, as listed in Ref. 13.

### 3. Computational Experiments

All experiments were done on a Pentium 4 1.3-GHz personal computer using the following algorithm programmed in MATLAB with Image Processing Toolbox:

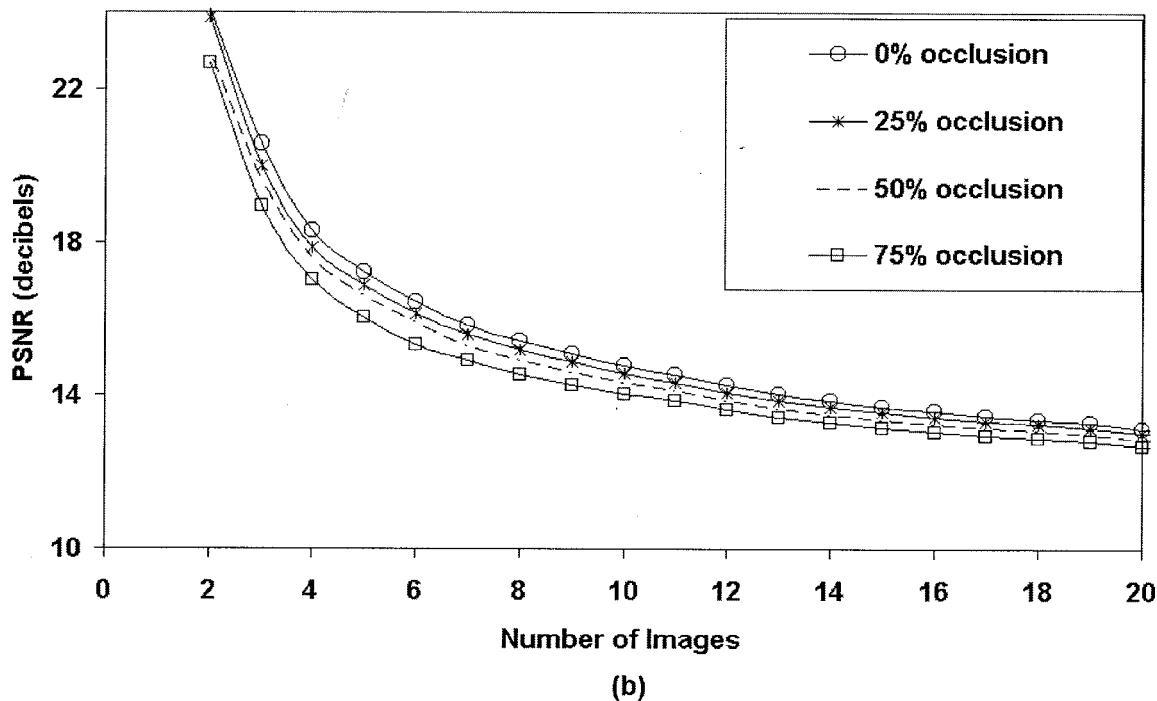
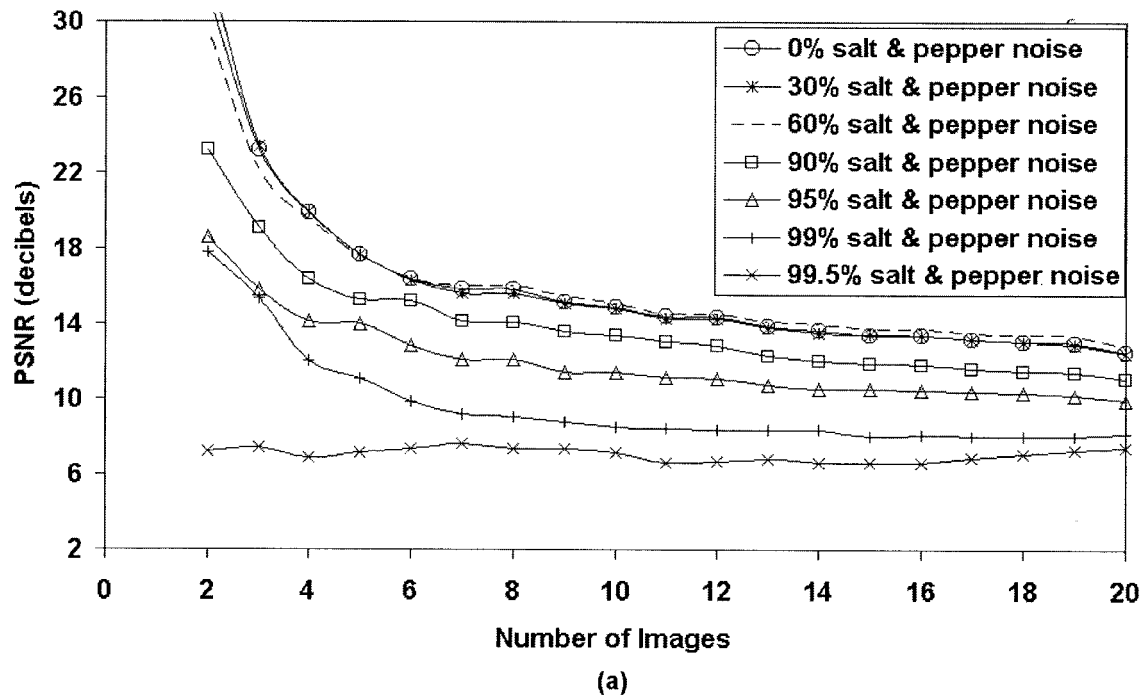


Fig. 1. Plots of peak signal-to-noise ratio of reconstructed image from “query-image” versus number of simultaneously-stored images of (a) Chinese pictograms and (b) fingerprints, where (a) query is a Chinese pictogram with salt-and-pepper noise, and (b) query is an occluded fingerprint.

- $P$  images with index  $k$  were encoded into  $\tilde{\mathbf{v}}^k = (\tilde{v}_1^k, \dots, \tilde{v}_N^k)$ , where a pixel's greyness is described by  $\tilde{v}_j^k \in [0, 255]$  ( $j = 1, \dots, N$ ).
- Images were preprocessed according to  $v_j^k = \tilde{v}_j^k - 1/N \sum_{j=1}^N \tilde{v}_j^k$  for each  $k, j$ . The resulting vector  $\mathbf{v}^k$  was then normalized to satisfy  $\sum_{j=1}^N (v_j^k)^2 = 1$ . Such normalized  $\mathbf{v}^k$  are assumed to be quantum implemented into plane wave/laser beam  $\psi^k$ .

- Memory matrix Eq. (1) was calculated (storage stage).
- Later, in the selective reconstruction stage, a new query/recall-key input (corresponding to the reference beam) was inserted. The network reacted as described in Eq. (3), or equivalently in Eq. (6). The query input was completed (if partial initially) or corrected (if corrupted) based on memo-



Fig. 2. (a), Original image; (b), original image (a) with 80% salt-and-pepper noise; and (c)–(g), image restored from memory of 10 different simultaneously stored fingerprints after presentation of the “query-image,” which is (c) whole original image (a), (d) 25%-occluded image (a), (e) 50%-occluded (a), (f) 75%-occluded (a), and (g) noisy image (b).

rized examples, and scaled back into the  $[0, 255]$  range.

Quality of reconstructed image  $\mathbf{v}$  was measured with peak signal-to-noise ratio (in dB; for 255 gray-values):

$$\text{PSNR} = 20 \log_{10} \left( \frac{255}{\text{RMSE}} \right),$$

$$\text{RMSE} = \left[ \frac{1}{N} \sum_{j=1}^N (v_j^{\text{original}} - v_j^{\text{reconstructed}})^2 \right]^{1/2}.$$

We found that reconstruction quality only slightly decreased with an increasing number of images stored simultaneously, and that this behavior was similar regardless of the type of stored images and the type and rate of deviation of the query image from the stored images. For two examples see Fig. 1. Compare these plots with Fig. 2, which demonstrates examples of image recovery from occlusion or noise. Indeed, the capability of selective reconstruction by use of memory is almost the same for different rates of degradation (occlusion or corruption with noise) of the query image or its deviation from the original stored image(s).

As evident from Fig. 2, the image that shared the most pixels with the query image was selected from the memory matrix and reconstructed (recognized), being disrupted (merely) by cross talk due to the nonorthogonality of the stored images. Such results, typical for associative nets and holography, were also found in the mixed-set experiment (Fig. 3). Here, three very different sets of 10 different-content images, i.e., with big intersets differences and small intraset differences, were simultaneously stored.

Cross-talk backgrounds can be seen in Figs. 3(d)–3(f), but the reconstructed images are not disturbed too much.

#### 4. Conclusions

Our simulations confirm Hopfield net’s capabilities. The novelty of our simulations is the reconsideration of Hopfield net’s characteristics in the age of powerful computers—early simulations of the 1980s had a limited resolution of patterns rather than images. Moreover, our original proposal of quantum-wave implementation opens a possibility of nets having up to an almost infinite size, and of processing of huge or high-resolution images. Therefore Hopfield net’s storage limitations and cross talk do not manifest (too) much for our practical needs. The first problem, memory-capacity of the Hopfield model’s being limited (to  $P \doteq 0.14N$ ), is much reduced with the possibility of an astronomically big  $N$ . The second problem, cross talk, is reduced since images with a huge number of pixels are with high probability almost orthogonal. A summary of the proof: The probability distribution of values of the scalar product (SP) converges to Gaussian distribution, owing to the Central Limit Theorem, which can be applied for scalar product  $\langle \psi^a, \psi^b \rangle$  if the components of  $\psi$  are random. The Gaussian distribution has zero mean, so  $\langle \psi^a, \psi^b \rangle = 0$  (mean SP) and  $\sigma_{\text{SP}}^2 = R/N \rightarrow 0$  (SP variance) if  $N \rightarrow \infty$  ( $R$  is a limited real number dependent on possible values of  $\psi_j^k$ ).<sup>24</sup> Then, orthogonality is thus most probable.

Instead of plane waves, images could be encoded into Gabor wavelets, which are similar to quantum wave packets. Other possible (great) improvements will be studied in the future.

So why should one go to the trouble of doing opti-

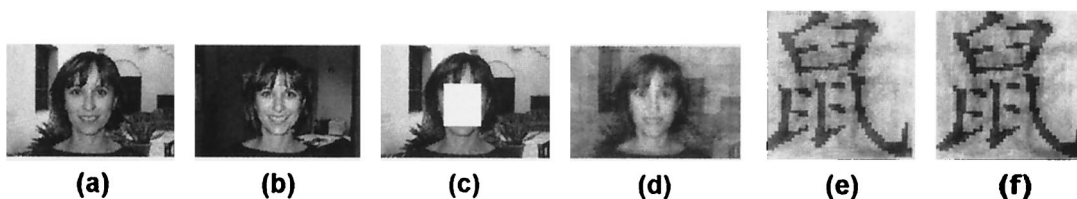


Fig. 3. Reconstruction from 30 simultaneously stored images (10 different Chinese pictograms and 10 different fingerprints as on Fig. 2(a) and 10 different face poses, such as in (a) and (b). “Query” (c) triggers reconstruction (d). (e) and (f), reconstructions from 25%- and 50%-occluded “query”-pictogram.



cally and quantum mechanically what works so well in the digital analog of such a quantum optical processor? There are two distinct kinds of benefits that stem from doing most of the calculations virtually, i.e., in the wave domain, and detecting only the final result. First, there is an energy advantage. Bennett and Landauer<sup>25</sup> pointed out that physical logic gates that are required in conventional computers must dissipate at least an amount of energy  $kT \ln 2$  at temperature  $T$  for each binary operation ( $k$  is the Boltzmann constant). Actual logic gates typically dissipate far more energy, say  $10^5$  kT per bit. Caulfield *et al.*<sup>26–28</sup> showed that operations done optically and virtually and never measured cost no energy, so if most of the operations are virtual, the energy cost per operation can drop below kT. Even  $10^5$  kT is not very much energy, but if the system is to produce many bits per second, the power dissipated can be quite large. Fast electronic computers run hot. Fast optical computers do not. Second, Caulfield *et al.* failed to notice that real, i.e., electronic, operations tend to limit the throughput speed of computations. Virtual operations, on the other hand, work at whatever bandwidth the input and the readout dictate. They themselves do not limit the speed. Quantum optics offers the possibility of performing some of the operations virtually without involving electronic gates. Operations performed virtually, in the wave domain, have the advantage of not causing either energy dissipation or process speed limitations.

Our quantum-holographic proposal has clear advantages over other proposed quantum associative memories,<sup>3–8</sup> based on the mainstream of the quantum computing science using quantum-implemented logic gates, in the sense of simplicity, miniaturization, natural physical realizability of associative processing, memory capacity and dimensionality of data (specifically, size and resolution of images). Quantum-gate models<sup>3–8</sup> are, however, more compatible with the mainstream attempts for an universal-purpose quantum computer, not merely for associative tasks which our model masters.

M.P. thanks for discussions V. Bužek and C. Trugenberger. M.P. gratefully worked as an EU Marie Curie postdoc fellow (contract HPMF-CT-2002-01808).

## References

1. D. Bouwmeester, A. Ekert, and A. Zeilinger, eds., *The Physics of Quantum Information* (Springer, Berlin, 2000).
2. F. T. S. Yu and S. Jutamalia, eds., *Optical Pattern Recognition* (Cambridge U. Press, Cambridge, UK, 1998).
3. M. Andreucot and M. K. Ali, "Quantum associative memory," *Int. J. Mod. Phys. B* **17**, 2447–2472 (2003).
4. C. Trugenberger, "Probabilistic quantum memories," *Phys. Rev. Lett.* **87**, 067901 (2001).
5. C. Trugenberger, "Phase transitions in quantum pattern recognition," *Phys. Rev. Lett.* **89**, 277903 (2001).
6. D. Ventura and T. Martinez, "Quantum associative memory," *Info. Sci.* **124**, 273–296 (2000).
7. J. Howell, J. Yeazell, and D. Ventura, "Optically simulating a quantum associative memory," *Phys. Rev. A* **62**, 042303 (2000).
8. R. Schützhold, "Pattern recognition on a quantum computer," <http://xxx.lanl.gov/pdf/quant-ph/0208063> (3 Dec 2002).
9. M. Peruš and S. K. Dey, "Quantum systems can implement content-addressable associative memory," *Appl. Math. Lett.* **13**, 31–36 (2000).
10. J. Sutherland, "Holographic model of memory, learning and expression," *Int. J. Neural Sys.* **1**, 256–267 (1990).
11. R. Spencer, "Bipolar spectral associative memories," *IEEE Transac. Neural Netw.* **12**, 463–474 (2001).
12. A. V. Pavlov, "On algebraic foundations of Fourier holography," *Opt. Spectrosc.* **90**, 452–457 (2001).
13. C. Leichtle, W. Schleich, I. Averbukh, and M. Shapiro, "Quantum state holography," *Phys. Rev. Lett.* **80**, 1418–1421 (1998).
14. T. C. Weinacht, J. Ahn, and P. H. Bucksbaum, "Controlling the shape of a quantum wavefunction," *Nature* **397**, 233–235 (1999).
15. M. Peruš and H. Bischof, "Quantum-wave pattern recognition," in *Proceedings of the 7th Joint Conference on Information Sciences*, K. Chen, ed. (JCIS/Association for Intelligent Machinery, Durham, N.C., 2003), pp. 1536–1539.
16. H. Bjelkhagen and H. J. Caulfield, eds., *Selected Papers on the Fundamental Techniques in Holography* (SPIE Press, Bellingham, Wash., 2001).
17. W. Schleich, *Quantum Optics in Phase Space* (Wiley-VCH, Berlin, 2001).
18. A. Granik and H. J. Caulfield, "Quantum holography," in *Holography*, Vol. IS 8 of SPIE Institute for Advanced Optical Technologies Series (SPIE Press, Bellingham, Wash., 1990), pp. 33–38.
19. M. Peruš, "Neural networks as a basis for quantum associative networks," *Neural Netw. World* **10**, 1001–1013 (2000).
20. D. Smithey, M. Beck, M. Raymer, and A. Faridani, "Measurement of the Wigner distribution and the density matrix of a light mode using optical homodyne tomography," *Phys. Rev. Lett.* **70**, 1244–1247 (1993).
21. G. D'Ariano and P. Lo Presti, "Quantum tomography for measuring experimentally the matrix elements of an arbitrary quantum operation," *Phys. Rev. Lett.* **86**, 4195–4198 (2001).
22. D. Goswami, "Optical pulse shaping approaches to coherent control," *Phys. Reports* **376**, 385–481 (2003).
23. B. Travaglione and G. Milburn, "Generation of eigenstates using the phase estimation algorithm," *Phys. Rev. A* **63**, 032301 (2001).
24. G. Rigatos and S. Tzafestas, "Fuzzy learning compatible with quantum mechanics postulates," in *Proceedings of the 7th Joint Conference on Information Sciences*, K. Chen, ed. (JCIS/Association for Intelligent Machinery, Durham, N.C., 2003), pp. 1532–1535, sec. 2.
25. C. Bennett and R. Landauer, "The fundamental physical limits of computation," *Sci. Am.* **253**, 48–56 (1985).
26. H. J. Caulfield and J. Shamir, "Wave-particle duality processors: characteristics, requirements, and applications," *J. Opt. Soc. Am. A* **7**, 1314–1323 (1990).
27. H. J. Caulfield and J. Shamir, "Wave-particle duality considerations in optical computing," *Appl. Opt.* **28**, 2184–2186 (1989).
28. H. J. Caulfield, J. Shamir, J. Ludman, and P. Greguss, "Reversibility and energetics in optical computing," *Opt. Lett.* **15**, 812–814 (1990).